Open access • Journal Article • DOI:10.1088/0967-3334/36/8/1691

Heart beat detection in multimodal data using automatic relevant signal detection.

Thomas De Cooman, Griet Goovaerts, Carolina Varon, Devy Widjaja ...+2 more authors

Institutions: Katholieke Universiteit Leuven

Published on: 28 Jul 2015 - Physiological Measurement (IOP Publishing)

Topics: Detection theory and Noise (signal processing)

Heart Beat Detection in Multimodal Data Using Automatic Relevant Signal Detection

Thomas De Cooman[1,2], Griet Goovaerts[1,2], Carolina Varon[1,2], Devy Widjaja[1,2], Tim Willemen[1,2] Sabine Van Huffel[1,2]

1 STADIUS Center for Dynamical Systems, Signal Processsing and Data Analytics, Department of Electrical Engineering-ESAT, KU Leuven, Leuven, Belgium
2 iMinds Medical IT Department, Leuven, Belgium
Thomas De Cooman, Kasteelpark Arenberg 10 - bus 2446, 3001 Leuven, Belgium

E-mail: thomas.decooman@esat.kuleuven.be

January 2015

Abstract. Accurate R peak detection in the electrocardiogram (ECG) is a well-known and highly explored problem in biomedical signal processing. Although a lot of progress has been made in this area, current methods are still insufficient in the presence of extreme noise and/or artifacts such as loose electrodes. Often however not only the ECG is recorded, but multiple signals are simultaneously acquired from the patient. Several of these signals such as blood pressure, can help to improve the heart beat detection. These signals of interest can be detected automatically by analyzing their power spectral density or by using the available signal type identifiers. Individual peaks from the signals of interest are combined using majority voting, heart beat location estimation and Hjorth's mobility of the resulting RR intervals. Both multimodal algorithms showed significant increases in performance of up to 8.65% for noisy multimodal datasets compared to when only the ECG signal is used. A maximal performance of 90.02% was obtained on the hidden test set of the 2014 Physionet/Computing in Cardiology challenge.

Keywords: multimodal, R peak detection, ECG, blood pressure
Submitted to: *Physiol. Meas.*

1. Introduction

Continuous extraction of the heart rate and heart rate variability is crucial in multiple monitoring applications. Typically only the available ECG signal is used for its computation. It can however occur that this signal becomes too noisy or the electrodes can even become disconnected, possibly leading to false or missing heart rate information, which could have crucial effects on the monitoring efficiency.

In several monitoring applications other biomedical signals are also acquired simultaneously. Pulsatile signals such as blood pressure (BP) or signals with strong

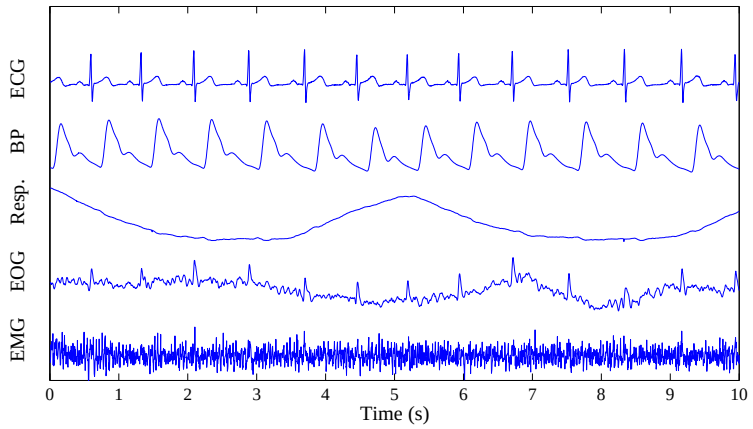

Figure 1. Example of a multimodal data segment. In this example the BP signal and the EOG signal with R peak interference can improve the performance of the heart beat detection in case the ECG signal would have been noisy.

R peak interference could be used for improved heart beat detection (see figure 1). The goal is to combine the heart beat information from all these signals in order to make a single decision about the R peak locations. This was also the subject of the 2014 Physionet/Computing in Cardiology challenge (from now on referred to as the 'challenge') to which the proposed methods were submitted (Moody et al. 2015).

Signal type identifiers (*ECG*, *BP*, etc.) were available in the used datasets (see section 2), but this paper proposes a method that is able to automatically detect these signals that can improve the heart beat detection. In this way the algorithm is able to detect signals with R peak interference (e.g. EEG, EOG) and deal with missing or erroneous signal type identifiers (IDs). This procedure and the methods for multimodal heart beat detection are described in section 3. Finally, the results are given and discussed in sections 4 and 5. A precursor of this paper has been published in De Cooman, Goovaerts et al. (2014).

2. Datasets and challenge information

An overview of the detailed challenge information, restrictions and data can be found in (Moody et al. 2015). In this paper the mentioned training set contains the 200 recordings that were available after the challenge, and the test set contains the 200 other remaining hidden recordings. It should however be noted that the discussed methods were initially developed with the use of only the initial challenge training set.

Because the initial available training set did not contain sufficient challenging examples (typical performance $> 99.85\%$), an extra dataset of 100 recordings was extracted from the MGH/MF Waveform database (Welch et al. 1991). These were extracted as the recordings between the 20th and 30th minute of recordings 001 to 107. Recordings 041, 043, 045, 047-049 and 083 were left out due to errors during reading of the original data/annotations. The time intervals were chosen to guarantee that correct

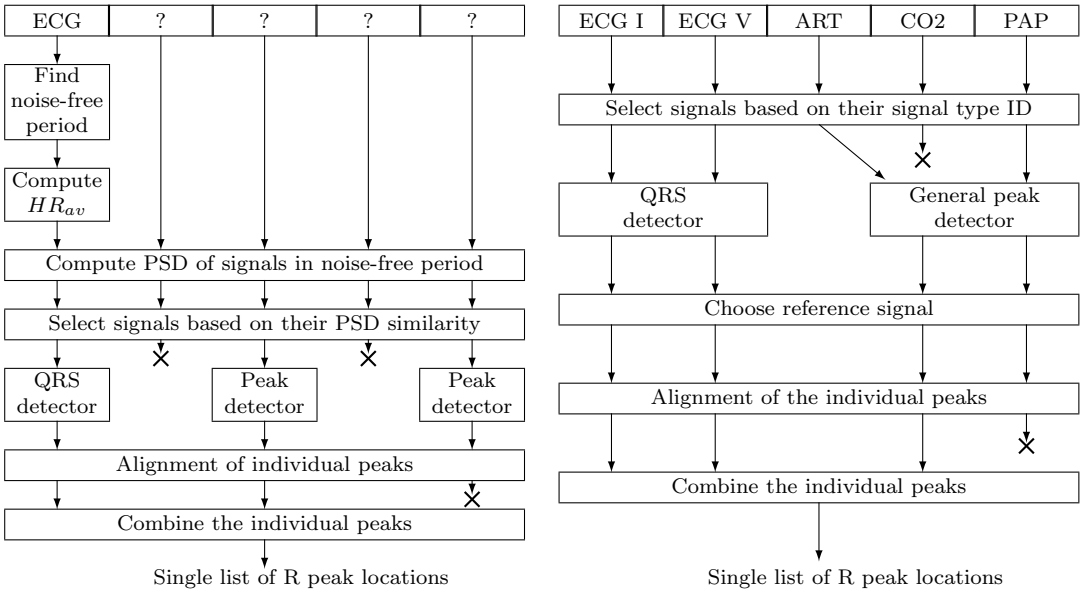

(a) MM_{NI} algorithm (b) MM_{WI} algorithm

Figure 2. Overview of the algorithms proposed in this paper. In the MM_{NI} algorithm (a), only the signal type of the first signal is certainly known (ECG). In the MM_{WI} algorithm (b), all available signal IDs are used. Crosses indicate after which steps signals can be removed from further processing.

reference annotations were available. These recordings typically contained additional ECG, pulmonary arterial pressure (PAP), arterial BP (ART) and central venous pressure (CVP) signals and can thus optimally profit from the methods discussed in this paper.

3. Methodology

Two algorithms for multimodal heart beat detection are elaborated in this paper (see figure 2). At first, a multimodal algorithm MM_{NI} that does not require the availability of signal type IDs (except for the known reference ECG signal) is discussed in sections 3.1 to 3.3. Section 3.4 describes an additional algorithm MM_{WI} that does use these signal IDs.

3.1. Automatic relevant signal detection using power spectral density similarity

At first, the potential signals of interest are selected automatically. These signals typically have the same periodic behavior as the ECG, which will be exploited in this procedure. With this procedure, there is no need for using the given (possibly false or missing) signal IDs, making the algorithm more robust when applying it on other databases. Pulsatile signals are examples of signals that need to be detected, but also other signals which contain R peak interference can improve the heart beat detection.

First, a noise-free segment of the ECG is selected based on a method described in Varon et al. (2012) as follows. The ECG is divided into k segments $C_i, 1 \leq i \leq k$, of

5 seconds and each segment is filtered using a bandpass Butterworth filter with cut-off frequencies at 1 Hz and 40 Hz. Next, the autocorrelation function (ACF) of each segment is computed. A similarity matrix S is then constructed with entries defined as

$$S_{i,j} = \frac{A_i^T A_j}{\|A_i\|\|A_j\|}, \qquad i,j = 1,2,...,k \tag{1}$$

with A_i the ACF of segment C_i. Now let

$$M_i = \sum_{j=1}^{k} S_{i,j}, \qquad i = 1,2,...,k \tag{2}$$

so that M_i gives an indication about the similarity between segment C_i compared to all other segments in the signal. We assume that the signal contains more noise-free than noisy segments, so a high similarity in a segment would indicate a noise-free segment. A period of l subsequent segments is then selected with maximal M_i values:

$$a = \arg\max_i \sum_{n=0}^{l-1} M_{i-n}, \tag{3}$$

with l chosen as the number of segments corresponding to 10% of the signal length (typically 1 minute). The resulting block of segments $C_{a-l+1,a-l+2,...,a}$ then forms the noise-free ECG period used in further processing.

The R peak detection algorithm from Yeh & Wang (2008) is then applied to this ECG segment and the average heart rate HR_{av} of this segment is obtained. Next, the normalized power spectral density (PSD) is computed for all signals in this time segment. Signals with the same periodic behavior as the ECG should contain a peak in their PSD around the average heart rate frequency HR_{av} (see figure 3). In order to get a more distinctive peak around HR_{av} in the ECG PSD, flattened ECG signals are used as input for the PSD computation. These flattened signals were found by subtracting the upper and lower secant envelopes from each other (Varon et al. In press 2015). The similarity (computed similarly as in (1)) between the PSD values in the interval [HR_{av}-0.3Hz, HR_{av}+0.3Hz] of the ECG signal and the other signals must exceed the threshold of 0.75 in order to be detected as a signal of interest. The value of this threshold is optimized heuristically using the available training set. Only these signals will be processed from now on. The procedure for detection of the noise-free ECG period was necessary in order to get a reliable estimate of the HR_{av} value.

3.2. Individual peak detection

In the next phase, heart beat locations are found for each signal of interest for the entire record length. For the first signal, a different QRS detection algorithm (*gqrs* from the WFDB toolbox) is used here compared to the one discussed in section 3.1 (Silva & Moody 2014). Although the latter resulted in a better performance, it was

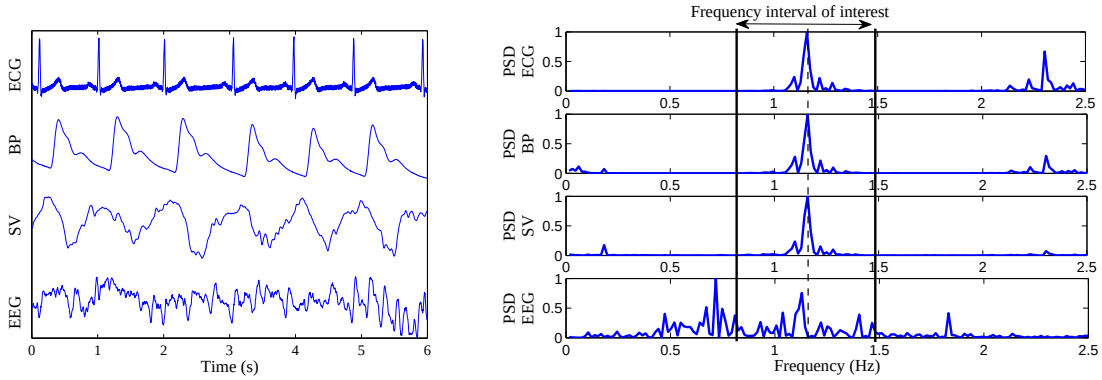

(a) Original signals. (b) PSD of signals.

Figure 3. Illustration of the automatic signal detection procedure. The left figure shows four signals during a 6 seconds epoch of the selected noise-free ECG period. The PSD values of all signals are shown in the right figure. The dotted line in the right figure indicates the average heart rate frequency HR_{av} in the selected noise-free period in the ECG signal. The frequency segment that is used for computing the correlation coefficient is marked by the solid vertical lines. In this example only the BP and stroke volume (SV) signal are selected as signals of interest.

computationally too expensive to run on the entire signal length. Therefore it was only executed on the noise-free ECG period to get a more reliable estimate of HR_{av}.

For the other signals, a basic general peak detection algorithm is used. First, an exponentially decreasing envelope e_{sig} is computed from each signal sig

$$e_{sig}(n) = \max_i sig(n - w + i)exp(-if_s^{-1}), \qquad i = 1, 2, ..., w \tag{4}$$

with f_s the sampling frequency of the signal and w the used window size, set here to $\lceil f_s/2 \rceil$. Heart beat locations are then detected if their corresponding envelope value is the highest value in a neighborhood of 300ms around its location. Despite its simplicity, the algorithm performed well on noise-free BP, stroke volume (SV) and ECG signals with positive peaks at a low computational load. By detecting the peaks of the signal envelopes, this method is more robust when finding peaks in additional ECG signals as the T peaks are less likely to be detected this way.

Because the peaks in the different types of signals do not occur at the same time as the ECG R peaks, the acquired peak positions need to be aligned with respect to the R peak locations before combining them in the next phase. The average delay between the peaks of the ECG and the other signals in the noise-free ECG period are computed and used for aligning each record separately. Derivation of the average delay is done by taking the most occurring delay between each signal and the reference ECG signal by computing the histogram of these delays. In this way, the algorithm can adapt to different kinds of signals of interest in a general way. If however the standard deviation of these delay values is too high (> 150ms), the corresponding signal is removed from further analysis. This may occur if a signal was falsely selected or if the corresponding peak locations are too inaccurate to increase the heart beat detection performance.

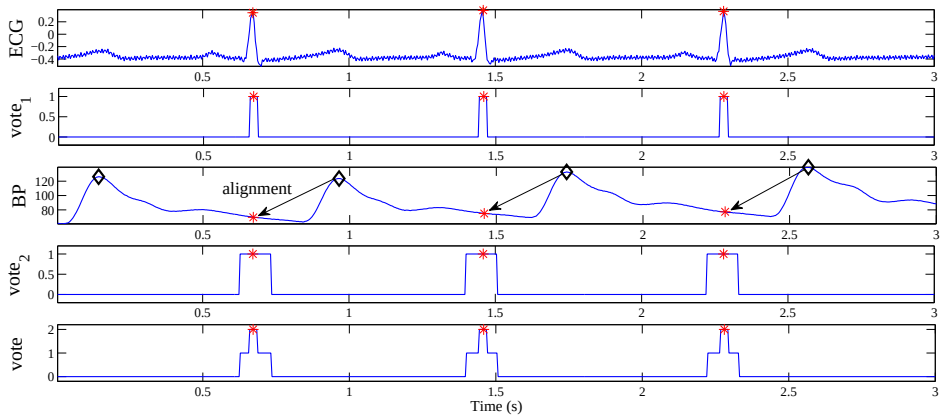

Figure 4. Illustration of the majority voting procedure for combining heart beats from different signals. Signals $vote_1$ and $vote_2$ indicate temporary versions of *vote* for each signal separately. The peaks from the BP signal are indicated by diamond symbols, the arrows indicate the peaks for this signal after alignment. Signal *vote* is defined as the sum of $vote_1$ and $vote_2$. The real R peak annotations are marked by an asterisk.

3.3. Combination of individual peak locations

Finally, the different individual peak locations from all signals need to be combined into a single list of R peak locations. This procedure runs in two phases. In a first phase, an initial list of R peak locations is found by using majority voting on the individual peak locations. This procedure is implemented here by defining a signal *vote*, which has the same length as the signals and all values are initialized at zero. For each peak location *loc* in each signal of interest, the values $vote(loc - window : loc + window)$ are increased with 1. For R peak locations coming from the known reference ECG signal, *window* equals 10ms, for other signals it is set to 50ms. This is due to the fact that the pulsatile signals tend to contain less accurate peak locations and could thus vary more compared to the corresponding R peaks in the ECG signal. This procedure is illustrated in figure 4. An initial set of peak locations *peaks* is then found by selecting peak values in *vote* which are greater than or equal to $\lfloor \#signals/2 \rfloor + 1$, with $\#signals$ the number of signals of interest.

In the second phase, this initial set of heart beat locations *peaks* is reinspected in a chronological fashion in order to see if heart beats have been missed. Define $RR(n)$ as the interval between $peaks(n)$ and $peaks(n+1)$. An estimation of the number of missing R peaks $est(n)$ in $RR(n)$ is defined as

$$est(n) = \begin{cases} 0 & : val(n) \leq 1.5 \\ 1 & : 1.5 < val(n) < 2.6 \\ 2 & : 2.6 \leq val(n) < 3.5 \\ round(val(n)) - 1 & : else \end{cases}$$

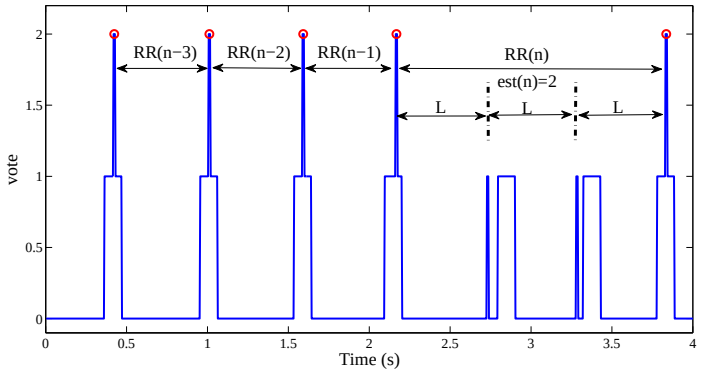

Figure 5. Illustration of the combination of peak locations of different signals. The red circles indicate the initial set of R peak locations *peaks*. In this case, peak locations from ECG (narrow peaks) and BP (wide peaks) are combined. The chained lines show the estimated R peak locations $estloc_2^n$, which lay near the ECG peaks. The ECG peak locations are thus added to *peaks* in this example.

with

$$val(n) = \frac{RR(n)}{median(RR(n-3:n-1))}$$

If $est(n) > 0$, further analysis of $RR(n)$ is required and peak locations in this interval need to be added. In this case, only peak locations originating from one signal can be added to *peaks*. The question remains from which signal to choose these peak locations in $RR(n)$. Let loc_i^n be the individual peak locations in $RR(n)$ from signal i. If at least one list of peak locations loc_i^n contains exactly $est(n)$ heart beats, one searches for one loc_i^n that follows this constraint and has a minimal Euclidean distance to the estimated missing beat locations $estloc_{est(n)}^n$. $estloc_j^n$ is defined here as a list of peak locations in $RR(n)$ containing j peaks, with peaks located so that they result in equally large RR-intervals in $RR(n)$ (see figure 5). When none of the peak location lists loc_i^n contains exactly $est(n)$ peaks, this procedure is repeated for $est(n) \pm 1$ and $estloc_{est(n)\pm1}^n$. If again no such list of beat locations is available or if $est(n) > 5$, the peak locations loc_i^n with the lowest variance in RR-intervals is chosen. Estimating the number of missing heart beats becomes too inaccurate if $est(n) > 5$ and is therefore avoided in this procedure. In these cases, loc_i^n are extended with $peaks(n-3:n-1)$ and $peaks(n)$ in order to check if these RR intervals fit in the surrounding RR values. When *peaks* is fully analyzed, it contains the final list of heart beat locations. An overview of the combining procedure is shown in algorithm 1.

3.4. Heart beat detection using signal type identifiers

A second version of the algorithm (called MM_{WI}) was also submitted for the challenge. In this version, the available signal type identifiers are used in order to define the potential signals of interest to be used for heart beat detection optimization. It is thus not able to detect signals which contain R peak interference, but is less likely to

Algorithm 1 Combining peak locations from different signals of interest

Input: loc_i with $1 \leq i \leq \#signals$ and $\#signals$ the number of signals of interest
Output: $peaks$ containing R peak locations
Construct $vote$ based on individual peak locations loc_i (see figure 4)
Find peak locations $peaks$ so that $vote(peaks) \geq \lfloor \#signals/2 \rfloor + 1$
for n=1:length($peaks$) **do**
  $RR(n) = [peaks(n), peaks(n+1)]$
  Estimate number of missing peaks $est(n)$ in $RR(n)$
  Define loc_i^n as the individual peak locations from signal i in $RR(n)$
  if $est(n) < 6$ **and** $\exists c \in [1, \#signals] : length(loc_c^n) = est(n)$
    $b = \arg\min_c \|estloc_{est(n)}^n - loc_c^n\|^2$
  else if $est(n) < 6$ **and** $\exists c \in [1, \#signals] : length(loc_c^n) = est(n) \pm 1$
    $b = \arg\min_c \|estloc_{est(n)\pm 1}^n - loc_c^n\|^2$
  else
    $b = \arg\min_i \text{var}(\text{diff}(loc_i^n))$, $i \in [1, \#signals]$
  end if
  add loc_b^n to $peaks$
end for

miss detection of signals with pulsatile signal IDs. The flow chart of this algorithm is shown in figure 2(b) and follows these steps:

(i) First the signals of interest are detected by searching for signal IDs containing the string 'ECG', 'BP', 'PLETH', 'PAP', 'ART', 'PPG' or 'pressure'. These signals were chosen as they typically yield robust information about the heart beat locations and the general peak detector performed well on these signals. SV and CVP signals were left out as they too often had too much variance in their peak locations, most often leading to a decrease in performance.

(ii) R peaks in signals with ECG IDs were computed by means of the *gqrs* algorithm because of its limited computational load. Heart beats in the other signals were detected by the general peak detector described in section 3.2.

(iii) It can occur that the first signal is not trustworthy as a reference signal for peak alignment. This is typically the case if the first signal is too noisy over a big part of the length. Therefore it is possible to change the reference signal in this method. It is chosen as the signal that has the lowest Hjorth's mobility in its heart rate values (Hjorth 1970). This parameter gives a good indication about the smoothness of the resulting tachogram. Non-ECG reference signals are aligned towards the R peak locations by using standard delay values for it's signal type (250ms for PAP, 200ms for other pulsatile signals).

(iv) All peak locations are aligned to these reference peak locations by computing the average delays over the entire signal length (similar to in MM_{NI}). Signals with a too large standard deviation ($>$ 150ms) on these delays are removed from the list of signals of interest.

(v) Different peaks are combined as discussed in section 3.3.

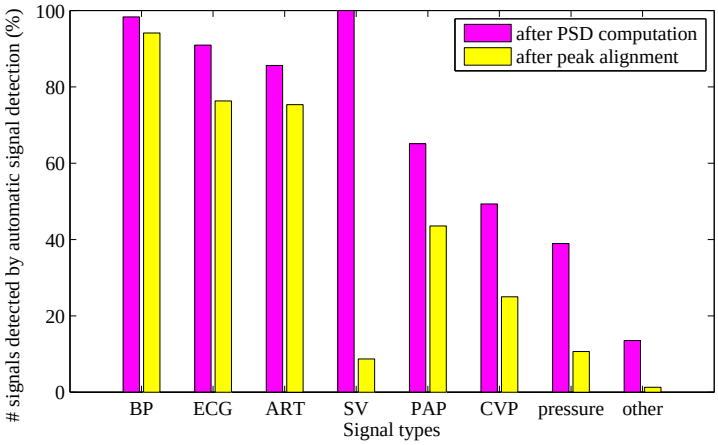

Figure 6. Percentages of signals with given identifier that are detected by the proposed method for automatic signal detection. The first bars indicate the sensitivity percentages of each signal type after inspecting the PSD similarity (see section 3.1), the seconds bars indicate the percentages of used signals after removing the signals with too high variability in delay values (see section 3.2).

4. Results

4.1. Automatic signal detection

The correctness of the automatic detection of signals of interest was evaluated on the challenge training set and the mentioned subset of the MGH/MF dataset (see figure 6). It should be noted that some of these assumed signals of interest might actually be too noisy to use, so the actual sensitivity values of useful signals are a bit higher.

As indicated, the signals that were used for the final beat locations were chosen in two steps. In the first step the similarity of the PSD values was used in order to get a first list of signals of interest. The most important signals of interest (BP, ECG and ART) are correctly detected in at least 91% of the cases after this first step.

Additional signals of interest were removed if the found alignment delays between the signals had a too high variance. The loss in detection sensitivity is limited here for the most important types of signals. The sensitivity drop is however larger for the CVP and PAP signals, and almost none of the SV signals are remained for further processing after this step. After this procedure, 10 non-pulsatile signals remained for further processing. All of them were however signals with R peak interference, so no signals were falsely selected for the final heart beat computation.

4.2. Multimodal heart beat detection

The performance of the different heart beat detection algorithms is evaluated by using the sensitivity (Se) and positive predictive value (+P) of the detected R peaks. R peak positions were labeled as a true positive if they were within a distance of 150ms of the correct reference annotations. Two variants of both measurements are used here.

Table 1. Results (in %) for the different proposed methods for multimodal heart beat detection. Also the results for the other final official top 5 challenge entries and for the unimodal *gqrs* algorithm are shown. $MM_{NI} - limited$ and $MM_{WI} - limited$ indicate the limited versions of both algorithms which can only use two signals. The last column indicates the average performance over both discussed datasets.

	Challenge training set			MGH/MF subset			Overall
Method	Se_{gr}	$+P_{gr}$	Av	Se_{gr}	$+P_{gr}$	Av	Av
gqrs	94.11	91.00	92.55	83.25	94.32	88.78	91.30
MM_{NI}	94.60	92.36	93.48	90.76	96.71	93.73	93.56
MM_{WI}	**95.40**	93.32	**94.36**	97.11	97.75	97.43	**95.38**
$MM_{NI} - limited$	95.04	92.32	93.68	89.31	96.66	92.98	93.44
$MM_{WI} - limited$	93.99	93.09	93.54	93.14	96.83	94.99	94.02
Johnson et al. (2014)	93.91	92.48	93.20	92.37	92.15	92.26	92.88
Vollmer (2014)	93.54	**94.61**	94.07	**97.22**	**97.96**	**97.59**	95.25
Gieraltowski et al. (2014)	94.22	93.29	93.75	78.77	95.80	87.29	91.60
Teo et al. (2014)	93.09	92.10	92.60	82.89	94.67	88.78	91.32

Table 2. Results for the different proposed methods for multimodal heart beat detection on the hidden challenge test set. The old version of the MM_{WI} algorithm is the algorithm as described in De Cooman, Goovaerts et al. (2014).

Method	Se_{gr} (%)	$+P_{gr}$(%)	Se_{av} (%)	$+P_{av}$(%)	Ov(%)
$MM_{WI} - limited$ (old)	89.49	86.06	87.09	87.78	87.60
$MM_{WI} - limited$	**90.74**	**90.15**	**89.59**	**89.62**	**90.02**
$MM_{NI} - limited$	88.96	87.52	86.44	85.30	87.05

Se_{gr} indicates the sensitivity over the entire dataset, whereas Se_{av} indicates the average sensitivity over the recordings (similar for $+P_{gr}$ and $+P_{av}$). The overall performance (Ov) is defined as the average of these 4 measurements (Moody et al. 2015). The average performance (Av) is the average of Se_{gr} and $+P_{gr}$.

Table 1 shows the results from both mentioned algorithms on the training set and the subset of the MGH/MF database. Because the Physionet server had a restricted processing time for each entry, which typically only allowed peak detection in two signals, also limited versions of the algorithms were elaborated that use maximally two signals (called $MM_{NI} - limited$ and $MM_{WI} - limited$). These two selected signals are the reference ECG signal and the first detected signal of interest (either by using the PSD procedure in $MM_{NI} - limited$ or using the signal ID's in $MM_{WI} - limited$).

The results of the discussed algorithms and the original versions of these algorithms as discussed in De Cooman, Goovaerts et al. (2014) on the hidden test set, are shown in table 2. The initial version of the algorithm ended third in the last stage of the official challenge (Moody et al. 2015). A maximum score of 90.02% was found for the $MM_{WI} - limited$ algorithm on the hidden test set of the challenge.

The results of the other official top 5 entries from the 2014 Physionet/Computing in Cardiology challenge (Goldberger et al. 2000) and the unimodal *gqrs* algorithm (applied

on the available ECG signal) are also shown in table 1.

All proposed multimodal algorithms result in a clear performance increase compared to when only the ECG signal is used. Especially for the subset of the MGH/MF database this increase is significant: a performance increase of 8.65% and 5.06% for the MM_{WI} and MM_{NI} algorithms. The performance gain in the challenge training set is a bit smaller as half of this dataset (the original training set) already had a performance of around 99.6% for the *gqrs* algorithm, which did not leave much room for further improvement. A similar trend is noticeable for the limited algorithm versions, but most often with a lower performance increase.

5. Discussion

5.1. Automatic signal detection

During the first phase of the automatic signal detection procedure, typical reasons for missing the most important signals (ECG, BP and ART) were noisy (reference) signals or too many false R peak detections in the reference ECG signal. Missed detections of PAP and CVP signals were typically due to too much interbeat variation in these signals, which would otherwise lead to bad peak detection in further processing. Some EEG, EOG and EMG signals contaminated with R peaks were also detected with this method, which would not be possible with the MM_{WI} algorithm. A few low-frequency signals (e.g. respiration) were however falsely detected if they accidentally had a harmonic frequency peak at HR_{av}.

After the second stage of the algorithm, most signals with inaccurate heart beat locations were removed from the signals of interest. This can be seen in the big drop in detection sensitivity for the SV signals, and to a lesser extent for the CVP and PAP signals. Some important signals were however also dropped, either by the absence of periodic positive peaks or due to bad R peak detection, but the sensitivity drop for these signals was significantly lower.

The introduced method for automatic signal detection does not only detect most of the pulsatile signals, but also discovered new signals that can improve the heart beat detection. Apart from that advantage, other advantages of this approach are that the algorithm can also be used reliably if

- there are no signal type identifiers available in the database;
- signal type errors can often occur; or
- the way of signal identifying is unknown or uncertain (full names versus abbreviations for IDs, different types of abbreviations, different language, etc.).

The method however still requires the availability of 1 known ECG signal.

One of the main drawbacks of this method is that it assumes that all signals are noise-free during the selected noise-free ECG period. This is however not always the case. A first problem is that the approach for detecting the noise-free ECG period assumes that the majority of the ECG is noise-free, but this is however not the case

in some recordings. This could possibly lead to missing all potential signals of interest in that recording. A second problem is that the approach also assumes that when the reference ECG signal is noise-free, all other signals are also noise-free, which is not always true. A signal that is temporarily detached during the noise-free ECG period might be useful outside this period, but will not be selected as a signal of interest. A potential solution to the latter problem would be to apply the same method for detection of a noise-free period on each signal instead of only the known ECG. To see if a signal $s, 2 \leq s \leq N$, with N the number of signals in the recording, is a signal of interest, one can combine both similarity matrices in order to find a period in time in which both signals have a maximal similarity

$$a_{(s)} = \arg\max_{j} \sum_{n=0}^{l-1} M_{j-n}^{(1)} + M_{j-n}^{(s)} \tag{5}$$

The PSD values and their similarity to the ECG PSD values can then be computed in this segment. This procedure is left for future work. It however still requires the reference ECG signal to be noise-free for at least 50% of the signal.

5.2. Multimodal heart beat detection

In both datasets and both algorithm versions, MM_{WI} resulted in a better performance than MM_{NI}, but this difference was minimal in case of the limited versions. Several reasons for the difference in performance can be found. In case the majority of the reference ECG signal is noisy, a noisy ECG segment is more likely to be selected. This can produce errors in HR_{av}, possibly leading to missing all potential signals of interest or aligning towards bad R peak locations. A second reason is the fact that MM_{WI} is able to switch the reference signal. By doing this, a noisy or disconnected ECG can be exchanged for another signal with a more logical RR sequence. The alignment step is therefore more reliable, typically leading to less shifted heart beat locations. By adding this procedure to the MM_{WI} algorithm, a performance increase of around 1.5% was found on the hidden challenge test set. MM_{NI} was however not able to find any peak location in 5 recordings in the hidden test set because of its dependency on the ECG signal. Finally, MM_{WI} is able to use the specific QRS algorithm *gqrs* on possible additional ECG signals in the MGH/MF database. MM_{NI} however had to use the general peak detector, which is less accurate and is not able to detect negative R peaks. If however the majority of the reference ECG is indeed noise-free, both algorithms have a very similar performance. For the initial challenge training set, MM_{NI} even worked slightly better as it was able to detect some extra signals with R peak interference, which was not possible with MM_{WI}.

The original version of the proposed algorithms was described in De Cooman, Goovaerts et al. (2014). The main differences of the current versions compared to the original version are the addition of the automatic selection of the reference signal (MM_{WI}), the lowering of the PSD similarity threshold (MM_{NI}) and fixing of some

programming bugs (MM_{NI} & MM_{WI}). By making these adjustments on the MM_{WI} algorithm, a performance increase of 2.42% was accomplished on the new hidden test set for the MM_{WI} algorithm (see table 2).

Compared to the other official top 5 challenge entries, both proposed limited methods would get a third place on the challenge training set. The difference with the better performing algorithms here is the fact that these use another R peak detector, which are probably better suited for ECG signals with pacemaker artifacts. The used *gqrs* algorithm is not able to deal well with these artifacts, typically leading to either shifted R peak locations or additional peaks for these artifacts. Beats from other signals could be aligned to these erroneous R peak locations, which can lead to large series of shifted R peak locations. However for the MGH/MF subset, only the algorithm proposed in Vollmer (2014) gives a better performance. The algorithm does not put a limit on the number of signals to be used, but as it is typically around 5 signals in this dataset, computing it might be too long for using it on the Physionet server. The non-limited version of the MM_{WI} algorithm however gives the best performance over both datasets.

It should be noted that a fairly high amount of false and missed R peak detections occurred due to the mentioned shifted R peak locations. These sometimes occur in large series of shifted peaks, but the resulting immediate heart rate measurements only differ in the beginning and end of these series. The intermediate heart rate values are most often correct in this case. Because typically only the heart rate values themselves are used in practice, the real error rate is even lower than the R peak detection error.

The proposed algorithms worked well during different observed arrhythmias, leading to a performance increase compared to unimodal heart beat detection. Because the algorithms try to find the most "logical" RR sequence in the available R peak locations, it can however occur that a wrong R peak location is chosen in case of a special beat (e.g. a premature beat). These special beats lead to an abnormal looking heart rate value compared to previous values, and might therefore not be preferred if a more smooth RR sequence can be obtained with another available R peak location from another signal. This however only occurs if the corresponding R peak locations from both signals do not resemble well and if at least one of the signals contains artifacts during this period. The number of these errors were however limited in the observed datasets. The presence of arrhythmia's does not interfere with the detection of signals of interest.

The general peak detection algorithm was rather basic in order to be able to detect peaks in multiple different signals of interest. Nevertheless it was able to give similar results as specific BP and R peak detectors in case of positive peaks and limited noise. If the specific BP detector from the WFDB toolbox would be used in the MM_{WI} algorithm, performance slightly decreased on the discussed training sets. More enhanced QRS and BP peak detectors could however be used in order to further optimize the performance.

6. Conclusion

The proposed multimodal algorithms were able to detect the R peaks more robustly compared to unimodal algorithms. The most important signals that can help to improve the R peak detection were reliably detected in at least 90% of the cases, and also other signals with strong R peak interference were detected with the proposed method. The individual peaks of the different signals of interest were successfully combined by a procedure containing majority voting, heart beat location estimation and Hjorth's mobility. Its performance can be further increased by optimizing the individual peak detection algorithms or by incorporating reliability scores to the different signals during the voting procedure. The methods could be used to improve R peak detection in several multimodal heart beat detection applications like in the ICU or for epileptic seizure detection using ECG in the hospital (De Cooman, Carrette et al. 2014).

Acknowledgments

Research supported by Research Council KUL: CoE PFV/10/002 (OPTEC), GOA/10/09 MaNet, PhD/Postdoc grants; FWO: PhD/Postdoc grants, G.0427.10N (Integrated EEG-fMRI), G.0108.11 (Compressed Sensing), G.0869.12N (Tumor imaging), G.0A5513N (Deep brain stimulation); IWT: PhD/Postdoc grants, TBM 080658-MRI (EEG-fMRI), TBM 110697-NeoGuard; iMinds Medical Information Technologies: SBO 2014, ICON NXT Sleep; Flanders Care Demonstratieproject Tele-Rehab III (2012-2014); Belgian Federal Science Policy Office IUAP P7/19 (DYSCO, Dynamical systems, control and optimization, 2012-2017); Belgian Foreign Affairs-Development Cooperation: VLIR UOS programs; EU RECAP 209G within INTERREG IVB NWE programme, EU MC ITN TRANSACT 2012 (no 316679), ERC Advanced Grant BIOTENSORS (no 339804), ERASMUS EQR Community service engineer (no 539642-LLP-1-2013); T. De Cooman, G. Goovaerts and D. Widjaja are supported by an IWT PhD Grant.

References

De Cooman, T., Carrette, E., Boon, P., Meurs, A. & Van Huffel, S. (2014). Online seizure detection in adults with temporal lobe epilepsy using single-lead ECG, *Proceedings of the 22nd European Signal Processing Conference (EUSIPCO), 2014*, IEEE, pp. 1532–1536.

De Cooman, T., Goovaerts, G., Varon, C., Widjaja, D. & Van Huffel, S. (2014). Heart Beat Detection in Multimodal Data Using Signal Recognition and Beat Location Estimation, *Proc. of the 41st Annual Computing in Cardiology (CinC2014)*, pp. 549–552.

Gieraltowski, J., Ciuchcinski, K., Grzegorczyk, I., Kozna, K., Solinski, M. & Podziemski, P. (2014). Algorithm for Detection of Heart Rate from Noisy Multimodal Recordings, *Proc. of the 41st Annual Computing in Cardiology (CinC2014)*, pp. 253–256.

Goldberger, A. L., Amaral, L. A., Glass, L., Hausdorff, J. M., Ivanov, P. C., Mark, R. G., Mietus, J. E., Moody, G. B., Peng, C.-K. & Stanley, H. E. (2000). Physiobank, physiotoolkit, and physionet components of a new research resource for complex physiologic signals, *Circulation* **101**(23): e215–e220.

Hjorth, B. (1970). EEG analysis based on time domain properties, *Electroencephalography and clinical neurophysiology* **29**(3): 306–310.

Johnson, A., Behar, J., Andreotti, F., Clifford, G. & Oster, J. (2014). R-Peak Estimation using Multimodal Lead Switching, *Proc. of the 41st Annual Computing in Cardiology (CinC2014)*, pp. 281–284.

Moody, B., Silva, I., Behar, J., Johnson, A., Oster, J., Clifford, G. D. & Moody, G. B. (2015). Editorial: Robust Detection of Heart Beats in Multimodal Data, *Physiological Measurement* **x**(x): x–x.

Silva, I. & Moody, G. (2014). An open-source toolbox for analysing and processing physionet databases in matlab and octave, *Journal of Open Research Software* **2**(1): e27.

Teo, S., Yang, B., Huan, D abd Christopher, M. & Su, Y. (2014). Robust Detection of Heart Beats using ECG, BP and EEG signals, *Proc. of the 41st Annual Computing in Cardiology (CinC2014)*, pp. 565–568.

Varon, C., Caicedo, A., Testelmans, D., B., B. & Van Huffel, S. (In press 2015). A novel algorithm for the automatic detection of sleep apnea from single-lead ECG, *IEEE Transactions on Biomedical Engineering (TBME)* .

Varon, C., Testelmans, D., Buyse, B., Suykens, J. A. & Van Huffel, S. (2012). Robust artefact detection in long-term ECG recordings based on autocorrelation function similarity and percentile analysis, *Engineering in Medicine and Biology Society (EMBC), 2012 Annual International Conference of the IEEE*, IEEE, pp. 3151–3154.

Vollmer, M. (2014). Robust Detection of Heart Beats using Dynamic Thresholds and Moving Windows, *Proc. of the 41st Annual Computing in Cardiology (CinC2014)*, pp. 569–572.

Welch, J., Ford, P., Teplick, R. & Rubsamen, R. (1991). The massachusetts general hospital-marquette foundation hemodynamic and electrocardiographic database–comprehensive collection of critical care waveforms, *Clinical Monitoring* **7**(1): 96–97.

Yeh, Y.-C. & Wang, W.-J. (2008). QRS complexes detection for ECG signal: The Difference Operation Method, *Computer methods and programs in biomedicine* **91**(3): 245–254.